Geochemistry of Basalt from Escanaba Trough: Evidence for Sediment Contamination

ALICÉ S. DAVIS[1]*, DAVID A. CLAGUE[1] AND WILLIAM M. WHITE[2]

[1]MONTEREY BAY AQUARIUM RESEARCH INSTITUTE, P.O. BOX 628, 7700 SANDHOLDT ROAD, MOSS LANDING, CA 95039-0628, USA

[2]CORNELL UNIVERSITY, DEPARTMENT OF GEOLOGICAL SCIENCES, SNEE HALL, ITHACA, NY 17853-1504, USA

Mid-ocean ridge basalts (MORBs) erupted in Escanaba Trough, the southernmost segment of the Gorda Ridge, have greater isotopic and geochemical variability than those from the remainder of the ridge. Samples from the sediment-free northern sites in the trough are depleted normal-MORB similar to those from the northern Gorda Ridge. However, samples from the sediment-covered portion of the trough are significantly enriched in incompatible elements, and Sr, Nd and Pb isotopic ratios are shifted toward the composition of local sediments. Pb isotopic ratios, in particular, lie on a mixing line with local sediments. Assimilation–fractional crystallization (AFC) calculations suggest that 25–40% fractional crystallization coupled with assimilation of 1–2% of local sediments can produce the enrichment observed for some Escanaba basalts. Variations in the amount of enrichment of elements with similar incompatibility for comparably differentiated basalts, and uncorrelated isotopic ratios suggest variable amounts of assimilation of compositionally heterogeneous assimilants by parental magmas. Assimilation of sediment by MORB magmas probably resulted when laccolithic intrusions ponded at the sediment–basement interface beneath the thick sediment cover in the southern part of Escanaba Trough. Geochemical and isotopic evidence for contamination can be detected in these lavas because of the strong compositional contrast between the parental magma and assimilant. The depleted MORB magma and highly enriched sediment assimilant are end-member compositions that provide a sensitive indicator for the smallest amount of contamination of oceanic magma by crustal processes.

KEY WORDS: *assimilation; basalt; Escanaba Trough; lead isotopes; mid-ocean ridge*

INTRODUCTION

Crustal contamination of basaltic magmas is generally recognized for continental volcanoes (e.g. Taylor, 1980; Leeman & Hawkesworth, 1986; Glazner *et al.*, 1991). The composition, thickness, and low melting temperatures of continental crustal rocks facilitate assimilation that can be easily identified. However, the extent to which basaltic magmas are contaminated by oceanic crust is a topic of intense debate (e.g. Bohrson & Reid, 1995; Clague *et al.*, 1995; Eiler *et al.*, 1996; Bohrson *et al.*, 1996, and references therein; Thirlwall *et al.*, 1997). The debate has focused on distinguishing the chemical characteristics magmas acquire during ascent, crustal storage, and emplacement from those that have been used to identify heterogeneous mantle sources. For most ocean island volcanoes, the crustal components available to serve as contaminants are poorly characterized, but include the underlying altered oceanic crust, pelagic to hemipelagic sediment, and the hydrothermally altered volcanic edifice.

Mid-ocean ridge basalts (MORBs) are relatively uniform geochemically with depleted incompatible element and radiogenic isotope compositions compared with lavas from ocean island or continental volcanoes. However, excess chlorine content and Cl/K ratios in fresh MORB glasses support the idea that MORB magmas may also be affected by assimilation of hydrothermally altered oceanic crust (e.g. Michael & Schilling, 1988; Michael & Cornell, 1996). Chlorine, like other incompatible elements, shows the greatest enrichment in strongly fractionated lavas that reside longer in shallow magma

chambers. MORBs with high-pressure liquid lines of descent (LLDs) do not show a similar Cl enrichment (Michael & Cornell, 1996), suggesting that assimilation occurs primarily in magmas stored in shallow, hydrothermally cooled reservoirs.

We present geochemical data for MORBs from Escanaba Trough, Gorda Ridge, where glasses from the sediment-covered southern portion show unusual geochemical enrichment and isotopic heterogeneity. These characteristics are modeled as resulting from assimilation of small amounts of local sediment, coupled with extensive crystal fractionation. The depleted MORB and strongly enriched sediment used in the models are end-member compositions that increase the 'signal-to-noise' ratio, resulting in the largest signature of crustal contamination for the smallest amount of contamination. The modeling determines the extent to which crustal processes may modify MORB magmas and identifies some chemical parameters, commonly interpreted to indicate heterogeneous mantle sources, that are most sensitive to modification by crustal processes.

GEOLOGIC SETTING

Escanaba Trough forms the southernmost segment of the Gorda Ridge (Fig. 1), extending 130 km northward from the Mendocino Fracture Zone at about 40°25′N latitude to a right-lateral offset near 41°35′N. The total spreading rate along the Escanaba Trough segment is ~2·3 cm/yr (Atwater & Mudie, 1973; Riddihough, 1980), which is characteristic of a slow-rate spreading center. Most of the rift valley is bordered by normal-faulted rift mountains up to 1500 m high. The valley floor is 3–5 km wide at the northern end and widens to 18 km near the junction with the Mendocino Fracture Zone. South of about 41°08′N latitude, the axis of Escanaba Trough is covered by turbidite and hemipelagic sediment (Moore & Sharman, 1970; Vallier et al., 1973; Karlin & Lyle, 1986; Morton & Fox, 1994). Terrigeneous sediments, originating at the North American continental margin, enter the valley at the southern end adjacent to the Mendocino Fracture Zone because topographic barriers in the form of rift mountains are absent in this region. Deep Sea Drilling Project (DSDP) Site 35, drilled slightly off axis in the central Escanaba Trough (Fig. 1), penetrated 390 m of Pleistocene turbidite sediment but did not reach volcanic basement (McManus, 1970).

Within the trough, discrete volcanic edifices uplift, and locally disrupt, the sediment cover (Denlinger & Holmes, 1994; Morton & Fox, 1994). Mesa-like hills, ~70–100 m high and ~1 km in diameter, are thought to be formed by laccolithic intrusions at, or near, the sediment–basement interface, 400–600 m below the sea floor (Denlinger & Holmes, 1994). Deformation of sediment generates sets of imbricated thrust and normal fault scarps exposing layers of sediments at the flanks of the hills (Zierenberg et al., 1994). Both thrust and normal faults channel hot seawater that precipitates large deposits of massive sulfide near the base of the escarpments (Denlinger & Holmes, 1994; Zierenberg et al., 1994). Apparently, uplift predated surface volcanic activity and basaltic feeders also followed fault traces to the sea floor, where eruptions produced lava flows on top of the sediments. These flows have been sampled in the sediment-covered southern Escanaba Trough.

Two of the larger volcanic sites were studied in detail by Morton & Fox (1994). The southernmost of these two sites, referred to as SESCA, is located at about 40°45′N, and the other site, referred to as NESCA, is located at about 41°00′N (Fig. 1). Seismic data indicate that the volcanic edifices at NESCA and SESCA have both intrusive and extrusive components and the sediments above the intrusions have been uplifted as much as 100 m in some places (Fig. 2). At both sites, exposed basaltic rocks are predominantly pillow basalts, although flat, folded, sheet and lobate flows also occur (Ross & Zierenberg, 1994). Flows typically appear to originate near the base of the uplifted sediment hills. Fissures and faults cut the flows and some fault scarps are in turn covered by basalt flows, indicating contemporaneous faulting and extrusion (Ross & Zierenberg, 1994). The flows at NESCA appear to be of similar age (Ross & Zierenberg, 1994), <10–20 ka based on ^{238}U–^{230}Th studies (Goldstein et al., 1992). Volcanic rocks were dredged from four additional, essentially sediment-free, sites north of NESCA, which we refer to as northern sites.

SAMPLING AND ANALYTICAL METHODS

Lava samples were recovered by dredging on R.V. S. P. Lee cruises L6-85NC, L2-86NC and L3-86NC, R.V. Kana Keoki cruise KK2-83NP, and by submersibles Alvin and Sea Cliff. Sediments were sampled using 3-m gravity cores on R.V. S. P. Lee cruises L5-86NC, L2-86NC, and L3-86NC. Forty-eight glassy rims of pillow and sheet flow fragments were selected for analysis by electron microprobe at the US Geological Survey in Menlo Park. The individual analyses and sampling details have been given by Davis et al. (1994). The 48 glasses were averaged into flow units if all elements were within analytical precision (Table 1). Selected glass samples were analyzed for chlorine using a sodalite standard (6·82% Cl). Analytical precision is 1–2% for major elements and 3–5% for minor elements. Precision for trace elements such as S and Cl is only about 10% and 30%, respectively, at these low concentrations. The interior of one basalt (Alv-2039-2) and sediments from Escanaba Trough were analyzed
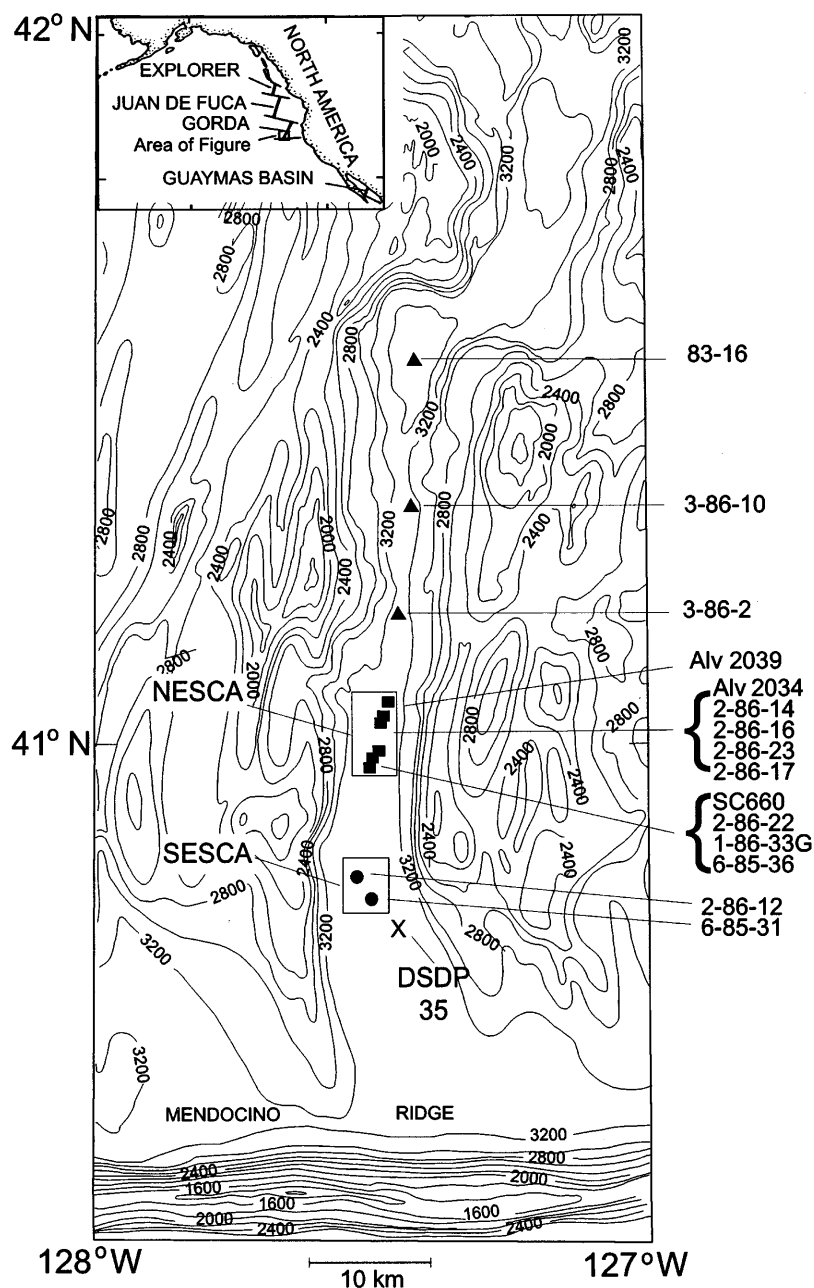
Fig. 1. Bathymetric map of Escanaba Trough showing sample locations and DSDP Site 35. NESCA and SESCA sites are indicated. Inset map shows location of oceanic ridge segments in the northern Pacific Ocean.

for major and some trace elements by X-ray fluorescence (XRF) in the Analytical Laboratory of the US Geological Survey in Denver.

Rare earth elements (REEs) on a representative set of basalt and sediment samples were analyzed by inductively coupled plasma mass spectrometry (ICP-MS) in the same place. Methods, precision and accuracy have been described by Lichte *et al.* (1987). Six samples were analyzed

for $^{87}Sr/^{86}Sr$, $^{143}Nd/^{144}Nd$ and Pb isotopic composition at Cornell University. Precision and accuracy of the methods have been given by White *et al.* (1990, and references therein). Oxygen isotope analyses were performed on eight selected samples at the US Geological Survey in Menlo Park. Oxygen was extracted by reaction with ClF_3 at 550°C in nickel bombs using methods similar to those described by Clayton & Mayeda (1963). All
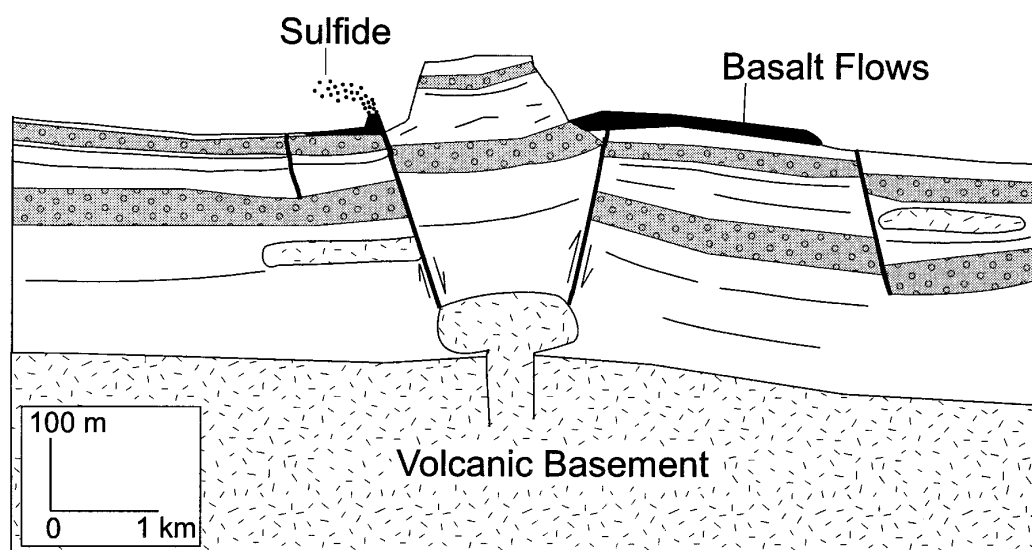
Fig. 2. Schematic cross-section showing uplifted sediment hill in Escanaba Trough as a result of magma intrusion. Faults provide pathways for basalt flows and for hydrothermal fluids, which form massive sulfide deposits at the base of the hill. Modified from Morton & Fox (1994).

oxygen isotope measurements were performed in duplicate and values are reported as permil deviation relative to SMOW (Standard Mean Ocean Water).

ESCANABA BASALT

Petrography

All samples appear fresh with mm- to cm-thick glass rinds; palagonite is thin or absent. One sample recovered by Alvin (Alv2039-2) has baked clay selvages on the glassy rinds. This glass is somewhat darker in color and less transparent than the other samples but shows no other visual evidence of devitrification. Except for plagioclase-phyric (>20%) samples from the northern sites (83-16, 3-86-10), samples are nearly aphyric or sparsely porphyritic with euhedral plagioclase and olivine microphenocrysts. Modal mineralogies of representative samples are included in Table 1. Minute (<200 μm), euhedral to subhedral spinel crystals occur in most samples but are especially abundant and in equilibrium with their host glass in NESCA samples. Olivine and plagioclase are texturally and compositionally similar to those from the northern Gorda Ridge (Davis & Clague, 1987, 1990) but spinel in NESCA samples is higher in TiO_2 and ferric iron (Fig. 3; Davis *et al.*, 1994) than spinel from the northern Gorda Ridge or typical N-MORB spinel from other slow-spreading centers (Sigurdsson & Schilling, 1976). Plagioclase in the high-K_2O sample (Alv2039-2) has measurable K_2O of ~0·06% (Davis *et al.*, 1994), compared with other plagioclase crystals from Gorda Ridge basalts, which have K_2O at or below detection limits (Davis & Clague, 1987, 1990).

Major element chemistry

The basaltic glasses from Escanaba Trough range from relatively primitive {*mg*-number [$100Mg/(Mg + Fe^{2+})$] ~67} to moderately fractionated (*mg*-number ~56, Table 1). The compositional range is similar to, but slightly less than that in basalt from the northern Gorda Ridge (*mg*-number 69–55; Davis & Clague, 1987). All glasses, except one, are low-K_2O N-MORB (Fig. 4a). Sample Alv2039-2 has a K_2O content of 0·43, is much higher than is typical for N-MORB and is the first such enriched composition reported from the Gorda Ridge. Besides a slightly elevated P_2O_5 content and lower, but variable, Na_2O abundance, this sample appears ordinary with respect to the other elements analyzed. As this sample has baked clay selvages on the glassy rind, a piece of the interior of the pillow was analyzed by XRF to determine if the high K_2O content is due to incipient secondary alteration. However, the interior of the pillow has only slightly lower K_2O content of 0·36% (Table 1) and the higher K_2O contents of the plagioclase confirm that the higher K_2O content is magmatic in origin. Although the other glasses have K_2O contents within the range typical of normal MORBs, at least two groups with distinct K_2O contents are apparent (Fig. 4a). All samples at the NESCA site have higher K_2O contents than is typical for samples with similar *mg*-numbers from northern Gorda Ridge. Unlike K_2O, TiO_2 content shows a narrower, well-defined trend with increasing *mg*-number (Fig. 4b). Despite considerable scatter, CaO/Al_2O_3 ratios generally increase with decreasing *mg*-number (Fig. 4c) compatible with primarily olivine and plagioclase fractionation. The higher CaO/Al_2O_3 ratio at comparable

*Table 1: Location and composition of Escanaba basalts*

	Northern sites								NESCA		
	83-16a	83-16b	3-86-10a	3-86-10b	3-86-10c	3-86-10d	3-86-2	3-86-3	Alv2039-2	Alv2039-2 (WR)	Alv2034
No. of samples:	2	1	6	1	1	2	2	2	2	1	2
Lat. (N):	41°31·3'	41°31·3'	41°26·9'	41°26·9'	41°26·9'	41°26·9'	41°20·1'	41°07·6'	41°05·3'	41°05·3'	41°01·0'
Long. (W):	127°27·4'	127°27·4'	127°25·4'	127°25·4'	127°25·4'	127°25·4'	127°26·5'	127°27·6'	127°28·5'	127°28·5'	127°29·5'
wt %											
SiO_2	50·3	50·0	51·0	50·6	50·7	50·6	50·2	50·3	50·4	49·8	50·8
Al_2O_3	14·6	15·3	15·4	15·1	15·9	15·1	16·4	15·8	15·5	15·1	15·1
FeO^T	10·9	9·69	9·39	10·6	9·73	10·2	8·83	9·31	10·4	10·3	10·0
MnO	0·21	0·18	0·17	0·20	0·20	0·19	0·16	0·17	0·19	0·19	0·20
MgO	7·10	7·80	8·16	7·40	7·30	7·57	8·92	8·13	7·52	7·67	7·28
CaO	11·2	11·6	11·8	11·3	11·7	11·6	12·0	11·6	11·3	11·5	11·4
Na_2O	2·56	2·80	2·51	2·77	2·83	2·70	2·46	2·67	2·49	2·69	2·78
K_2O	0·26	0·13	0·06	0·09	0·09	0·09	0·05	0·13	0·43	0·36	0·27
P_2O_5	0·21	0·11	0·12	0·16	0·12	0·14	0·09	0·16	0·27	0·22	0·23
TiO_2	1·92	1·58	1·30	1·71	1·51	1·62	1·07	1·44	1·74	1·76	1·64
S	0·13	0·11	0·10	0·12	0·11	0·12	0·09	0·10	0·12	—	0·11
Total	99·4	99·3	100·0	100·1	100·2	99·9	100·3	99·8	100·4	99·4	99·8
mg-no.	56·4	61·5	63·3	58·1	59·8	59·6	66·7	63·4	59·0	59·6	59·1
Gms	74%	72%	95%	79%	—	89%	98%	99%	98%	—	—
Ol	4%	<1%	<1%	2%	—	1%	1%	1%	<1%	—	—
Pl	22%	27%	4%	19%	—	10%	<1%	tr	<1%	—	—
Sp	tr	tr	tr	tr	—	tr	tr	tr	tr	—	—

Table 1: continued

	NESCA									SESCA	
	2-86-14	2-86-16	2-86-23	2-86-17a	2-86-17b	Sc 660	6-85-36	2-86-22a	2-86-22b	6-85-31	2-86-12
No. of samples:	2	2	4	2	1	1	9	1	1	2	2
Lat. (N):	41°00·7'	41°00·7'	41°00·5'	40°59·7'	40°59·7'	40°59·5'	40°59·0'	40°58·5'	40°58·5'	40°46·4'	40°45·9'
Long. (W):	127°29·7'	127°29·8'	127°29·8'	127°28·1'	127°28·1'	127°29·4'	127°30·2'	127°27·9'	127°27·9'	127°30·8'	127°32·7'
wt %											
SiO_2	50·7	50·8	50·8	50·8	51·1	51·0	50·3	50·8	51·0	51·7	51·2
Al_2O_3	14·8	14·8	14·8	15·1	15·2	15·3	15·4	15·4	15·1	14·8	15·5
FeO^T	10·3	10·4	10·3	10·0	10·6	9·87	9·71	10·1	10·2	8·68	8·47
MnO	0·19	0·20	0·20	0·18	0·20	0·18	0·19	0·18	0·19	0·18	0·17
MgO	7·25	7·35	7·15	7·32	7·36	7·87	7·58	7·47	7·68	8·34	8·37
CaO	11·3	11·2	11·3	11·3	11·2	11·3	11·4	11·2	11·1	12·6	12·7
Na_2O	2·79	2·82	2·84	2·72	2·28	2·77	2·71	2·79	2·82	2·45	2·38
K_2O	0·26	0·25	0·25	0·27	0·28	0·26	0·24	0·27	0·28	0·12	0·14
P_2O_5	0·22	0·21	0·21	0·21	0·22	0·21	0·18	0·20	0·21	0·10	0·12
TiO_2	1·73	1·73	1·74	1·68	1·80	1·61	1·54	1·66	1·73	1·06	1·03
S	0·12	0·12	0·12	0·11	0·12	0·11	0·11	0·11	0·11	0·10	0·10
Total	99·7	99·9	99·7	99·7	100·4	100·5	99·4	100·2	100·4	100·1	100·2
mg-no.	58·3	58·4	58·0	59·2	57·9	61·3	60·8	59·5	59·9	65·6	66·2
Gms	—	—	97%	96%	—	—	97%	99%	—	92%	93%
Ol	—	—	<1%	<1%	—	—	2%	<1%	—	1%	2%
Pl	—	—	2%	3%	—	—	1%	tr	—	7%	5%
Sp	—	—	tr	tr	—	—	tr	tr	—	—	—

FeO^T is total Fe calculated as FeO. *mg*-number is atomic $100Mg/(Mg + Fe^{2+})$, where $Fe^{2+} = 0.9Fe^T$. WR, whole-rock analysis by XRF. All others are glass analyses determined by electron microprobe. Modal composition calculated vesicle free, based on 1000 point counts. Gms, groundmass; Ol, olivine; Pl, plagioclase; Sp, spinel; —, not determined; tr, trace.
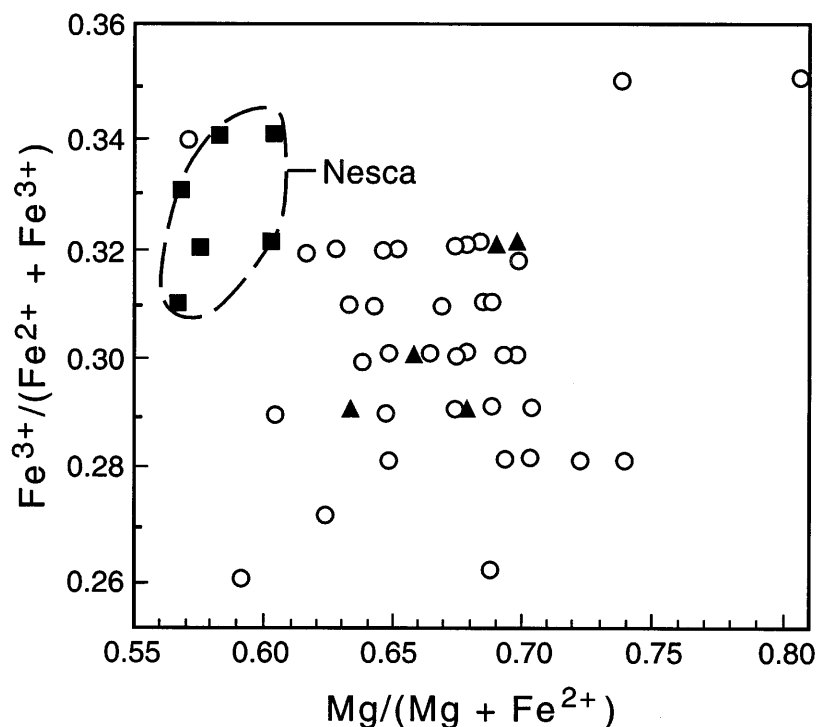
Fig. 3. Representative compositions of chromian spinel in Escanaba basalts show that spinel in NESCA basalts (■) has higher calculated ferric iron than typical for spinel in basalt from the northern sites in Escanaba Trough (▲) and in other Gorda Ridge basalts (○). Data from Davis & Clague (1987, 1990).

mg-number of SESCA glasses suggests greater amounts of plagioclase fractionation.

Trace element chemistry

Rare earth elements (REE) of selected Escanaba basalts are presented in Table 2 and chondrite-normalized profiles are shown in Fig. 5. The REE abundances are lowest in the least fractionated sample (*mg*-number ~67) from one of the northern sites (3-86-2). The chondrite-normalized profile of this sample is concave with pronounced light REE (LREE) depletion similar to that of un-fractionated lavas from the northern Gorda Ridge. The chondrite-normalized profile of the SESCA basalt does not have as concave a pattern as 3-86-2, although it has a similar *mg*-number (~66). This sample is higher in LREE and lower in heavy REE (HREE) and it has a significant negative Eu anomaly, indicating plagioclase fractionation. The NESCA basalts have higher overall REE abundances, as would be expected for more differentiated compositions (*mg*-number 60–56). However, the LREE are more enriched than in comparably fractionated basalt from the northern Gorda Ridge (Fig. 5), typically having $(La/Sm)_N >1$ (Table 2; Davis & Clague, 1987, 1990). The high K_2O sample (Alv2039-2) shows

no significant difference in REE pattern or abundances compared with lower K_2O NESCA samples. The REE composition of the glass from Alv2039-2 is also similar to the whole-rock interior (Table 2), indicating that any secondary alteration of the glass rind has not affected the REE. NESCA sample 2-86-17a has higher LREE abundances than the other NESCA samples and the profile is not parallel to the others. Several NESCA samples have very small negative Ce anomalies, whereas one has a small positive Ce anomaly (Fig. 5).

Sulfur concentrations range from 900 to 1300 ppm, a range similar to that observed for northern Gorda Ridge basalts (Davis & Clague, 1987, 1990). Chlorine ranges from ~30 ppm in the least fractionated sample from the northern site (3-86-2) to >100 ppm in samples from NESCA. However, in the glassy rim of the high-K_2O sample (Alv2039-2), Cl is inhomogeneously distributed and ranges from about 130 to 200 ppm, variation well beyond analytical uncertainty.

Isotopic composition

Sr, Nd, and Pb isotopic compositions (Table 2) are within the compositional range observed for Pacific MORB (Davis & Clague, 1987; White *et al.*, 1987; Church &
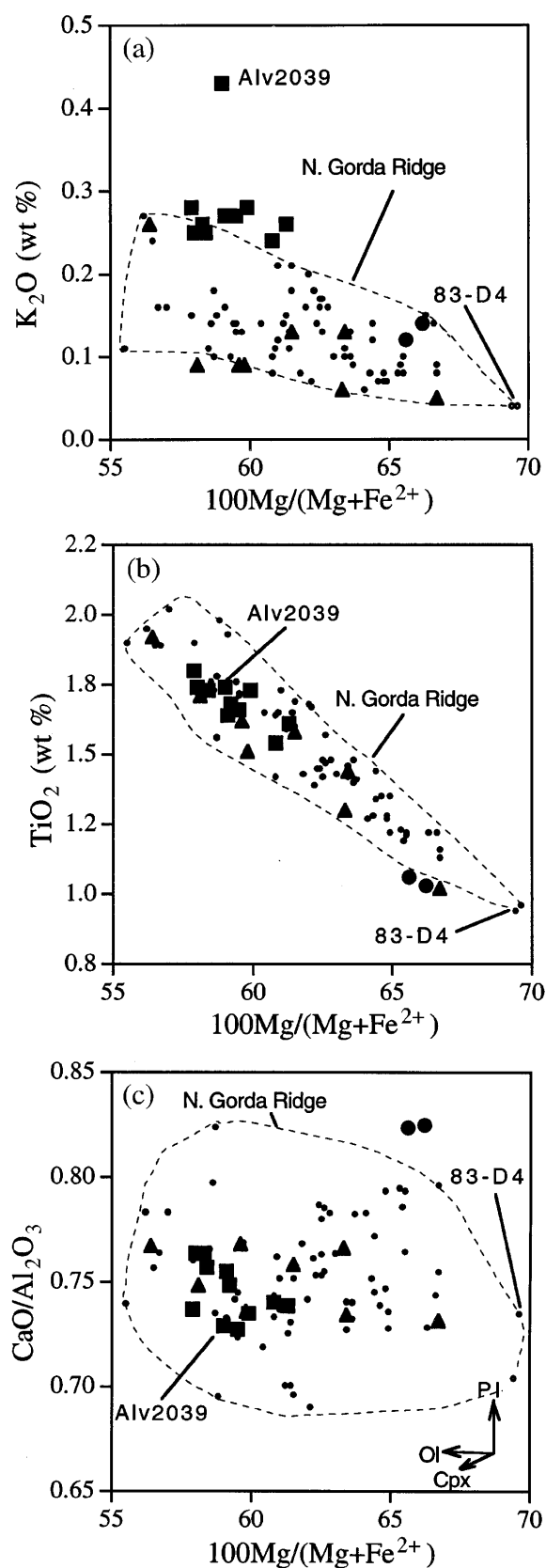
Tatsumoto, 1975). However, samples from the NESCA site have higher Sr and Pb and lower Nd ratios than other samples reported from the Gorda Ridge (Figs 6 and 7). On $^{208}Pb/^{204}Pb$ and $^{207}Pb/^{204}Pb$ vs $^{206}Pb/^{204}Pb$ plots (Fig. 6a,b) the Pb isotopic ratios of NESCA samples plot above the correlation line defined by northern Gorda Ridge basalts. $^{208}Pb/^{204}Pb$ appears well correlated with $^{206}Pb/^{204}Pb$; $^{207}Pb/^{204}Pb$ shows slightly more scatter. NESCA samples have significantly higher Sr and lower Nd isotopic ratios than other Gorda Ridge basalts but they are not well correlated with Pb isotopic ratios or each other (Fig. 6c, d). The Sr isotopic ratio of the SESCA basalt is slightly elevated with respect to northern Gorda Ridge basalts. Samples from the northern Escanaba sites fall within the field defined by northern Gorda Ridge basalts for all three isotopic systems.

Oxygen isotopes have a narrow compositional range ($\delta^{18}O$ +5·7 to +5·9 ± 0·1) for all samples except the high-K_2O glass rind of Alv2039-2, which has a significantly higher ratio of +6·5%. The interior of the pillow has $\delta^{18}O$ +5·9 like the other samples, indicating that the glass rim may have been affected by low-temperature alteration.

ESCANABA SEDIMENT

Sediments recovered with gravity cores in Escanaba Trough represent only the surficial upper 1% (3–4 m) of the thick sediment cover present in the southern part of the trough. The sediments are olive green to gray hemipelagic silty clay containing up to 25% volcanic glass and sulfides (Karlin & Lyle, 1986). Bulk chemical analyses, including the trace elements Sr, Ce and Pb, of over 170 sediment samples from the L5-86 cruise (Karlin & Lyle, 1986) were supplemented by a small number of additional sediment analyses, including the REE (Table 3).

The sediment compositions are highly variable from one core to another and within a given core. Pb concentrations range from 17 ppm to 119 ppm, Ce from
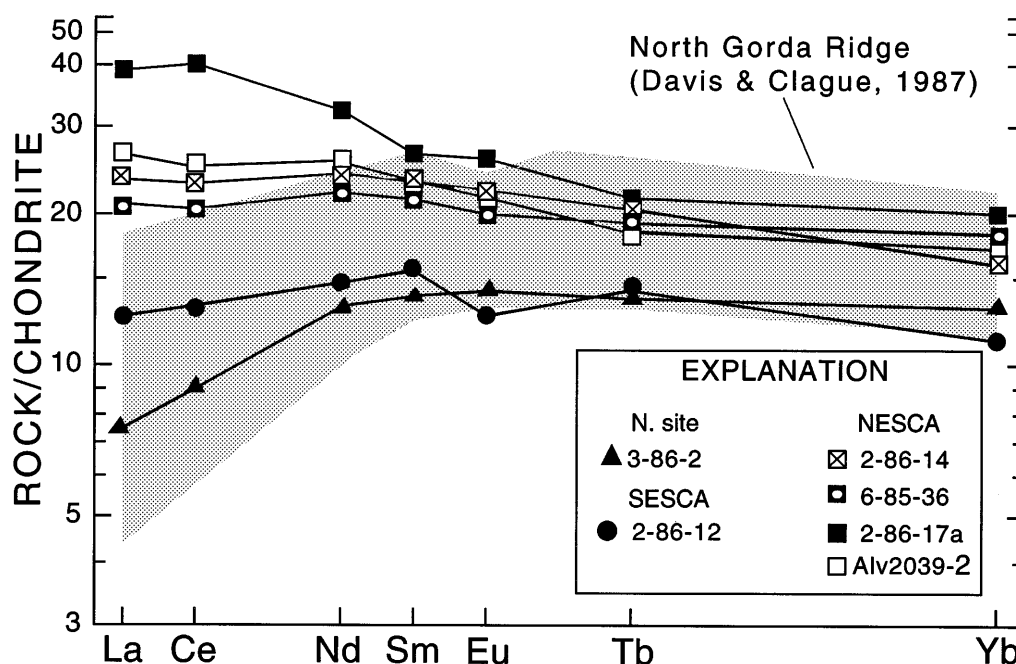
Fig. 4. Compositions of Escanaba basalts are shown in (a) K_2O, (b) TiO_2 and (c) CaO/Al_2O_3 vs *mg*-number plots. K_2O shows a large amount of scatter at a given *mg*-number. Basalts from northern Gorda Ridge (●) have a similar compositional range but high-K_2O compositions like that of Alv2039-2 are absent. Samples from NESCA have typically higher K_2O contents than comparably fractionated samples from other sites. TiO_2 vs *mg*-number shows a better defined trend, increasing with decreasing *mg*-number. CaO/Al_2O_3 ratios as a function of *mg*-number indicate different fractionation trends with different proportions of plagioclase and olivine. The high CaO/Al_2O_3 ratio of SESCA glasses suggests fractional crystallization of a large proportion of plagioclase. The most primitive composition recovered from Gorda Ridge (83-D4, Davis & Clague, 1987) is indicated. ●, SESCA; other symbols and data sources as in Fig. 3.

Table 2: Trace element and isotopic compositions of selected samples

	Northern sites				NESCA					SESCA
Sample:	83-16a	3-86-2	3-86-3	3-86-10a	Alv2039-2 (Glass)	Alv2039-2 (WR)	2-86-14	2-86-17a	6-85-36	2-86-12
(ppm)										
La	6.8	2.5	—	—	8.7	9.6	7.9	13.0	7.1	4.3
Ce	18.0	7.4	—	—	20.5	23.0	20.0	38.0	17.0	11.0
Nd	16.0	7.8	—	—	15.5	17.0	15.0	20.0	13.5	8.9
Sm	4.5	2.4	—	—	4.2	4.4	4.3	4.6	4.0	2.8
Eu	1.5	0.93	—	—	1.5	1.6	1.6	1.8	1.4	0.90
Tb	1.0	0.64	—	—	0.89	1.0	1.0	1.0	0.90	0.65
Yb	4.0	2.6	—	—	3.4	3.8	3.3	4.1	3.6	2.3
$(La/Sm)_N$	0.83	0.57	—	—	1.14	1.20	1.00	1.55	0.97	0.84
$(Ce/Yb)_N$	1.03	0.65	—	—	1.37	1.37	1.38	2.11	1.07	1.09
$^{87}Sr/^{86}Sr$	0.70261[1]	0.70248	0.70252	0.70246	0.70284	—	0.70274	0.70291	0.70284[2]	0.70259
$^{143}Nd/^{144}Nd$	—	0.513219	0.513238	0.513257	0.513155	—	0.513164	0.513148	0.513112	0.513252
$^{206}Pb/^{204}Pb$	—	18.351	18.353	—	18.511	—	18.645	18.695	18.701[3]	18.473
$^{207}Pb/^{204}Pb$	—	15.468	15.463	—	15.509	—	15.545	15.555	15.550	15.490
$^{208}Pb/^{204}Pb$	—	37.781	37.807	—	38.078	—	38.269	38.335	38.322	38.048
$\delta^{18}O$ (‰)	+5.9	+5.9	—	—	+6.5	+5.9	+5.8	+5.8	+5.7	+5.9
(ppm)										
Cl	50	30	40	30	130—200	—	90	100	90	60
Sr	—	98	—	—	170	—	—	—	139	127

[1]Data from Davis & Clague (1987). [2]Data from White *et al.* (1987). [3]Data from LeHuray *et al.* (1988). The $^{87}Sr/^{86}Sr$ ratios are relative to $^{87}Sr/^{86}Sr = 0.71024$ for the NBS 987 standard. Estimated analytical errors are ±0.000035 (2σ standard errors) based on replication of standards. The $^{143}Nd/^{144}Nd$ ratios are normalized to $^{146}Nd/^{144}Nd = 0.72190$, and are relative to 0.511855 for the La Jolla standard. Estimated analytical errors are ±0.000020. Pb isotope ratios were corrected for mass fractionation and are relative to values of $^{206}Pb/^{204}Pb = 16.937$, $^{207}Pb/^{204}Pb = 15.493$, and $^{208}Pb/^{204}Pb = 36.705$ for the NBS-981 Standard. Analytical uncertainties (2σ) are estimated at 206/204 = ±0.010, 207/204 = ±0.016, and 208/204 = ±0.035. Sr by XRF-EDS, Cl by electron microprobe. —, not determined.

Fig. 5. Chondrite-normalized REE distribution of Escanaba basalt shows a concave, LREE-depleted profile for the most primitive composition (3-86-2, *mg*-number ~67) from the sediment-free site in northern Escanaba Trough. The SESCA basalt, with a similar *mg*-number (~66) is less depleted in LREE and has a distinctive negative Eu anomaly, although it is only sparsely plagioclase-phyric. As would be expected from more differentiated compositions, NESCA basalts have overall higher REE abundances but variable, crossing REE profiles and more LREE enrichment than comparably fractionated compositions from the northern Gorda Ridge. The field of chondrite-normalized REE for northern Gorda Ridge basalt shown for comparison is from Davis & Clague (1987). Normalizing values of Haskin *et al.* (1968).

330 to >1500 ppm, and Sr from 234 ppm to 363 ppm (Karlin & Lyle, 1986) and are not well correlated with one another and show no trends with depth. Pb isotopic compositions of Escanaba sediment range from 18·968 to 19·092, 15·623 to 15·660, and 38·938 to 39·096 for 206/204, 207/204, and 208/204, respectively (Fig. 6; LeHuray *et al.*, 1987; R. Bouse, unpublished data, 1990). Oxygen isotopic compositions determined for the clay-size fraction of 18 samples from the same cores are also highly variable, with $\delta^{18}O$ ranging from +2·1 to +16·6 (Zierenberg & Shanks, 1994).

PETROGENESIS OF ESCANABA MORB

Chemical variation in MORB suites is typically interpreted to have resulted from fractional crystallization, magma mixing, degree and kind of partial melting, and mantle source heterogeneities. All of these processes apparently have been operative on the northern segments of the Gorda Ridge (Davis & Clague, 1987, 1990). Samples from the sediment-free sites in Escanaba Trough are indistinguishable from those of the northern Gorda Ridge but samples from the sediment-covered part of

Escanaba Trough are distinct. In particular, the high K_2O sample (Alv2039-2) has no counterpart from the northern sites.

Major element variations of Escanaba basalts can be explained by shallow depth crystal fractionation. Although variations in CaO/Al_2O_3 ratios with *mg*-numbers (Fig. 4c) suggest primarily olivine and plagioclase fractionation, crystal fractionation calculations require fractionation of significant amounts of clinopyroxene. The fractionated Escanaba glasses can be derived from a parental composition similar to the most primitive composition from Escanaba Trough (3-86-2) by fractionating ~25–40% of plagioclase, olivine, and clinopyroxene in approximate proportions of 2·5:1:1 [fractionation program of D. Geist (personal communication, 1992)]. As noted for many other MORB suites, clinopyroxene fractionation is required although modal clinopyroxene is rare or absent. Abundant large clinopyroxene crystals in xenolithic inclusions from the northern Gorda Ridge (Davis & Clague, 1990) provide evidence that clinopyroxene crystallization is an important process occurring at the margins of MORB magma chambers.

The REEs are particularly sensitive to petrogenetic processes and the highly variable, non-parallel chondrite-normalized patterns (Fig. 5) of Escanaba basalt suggest
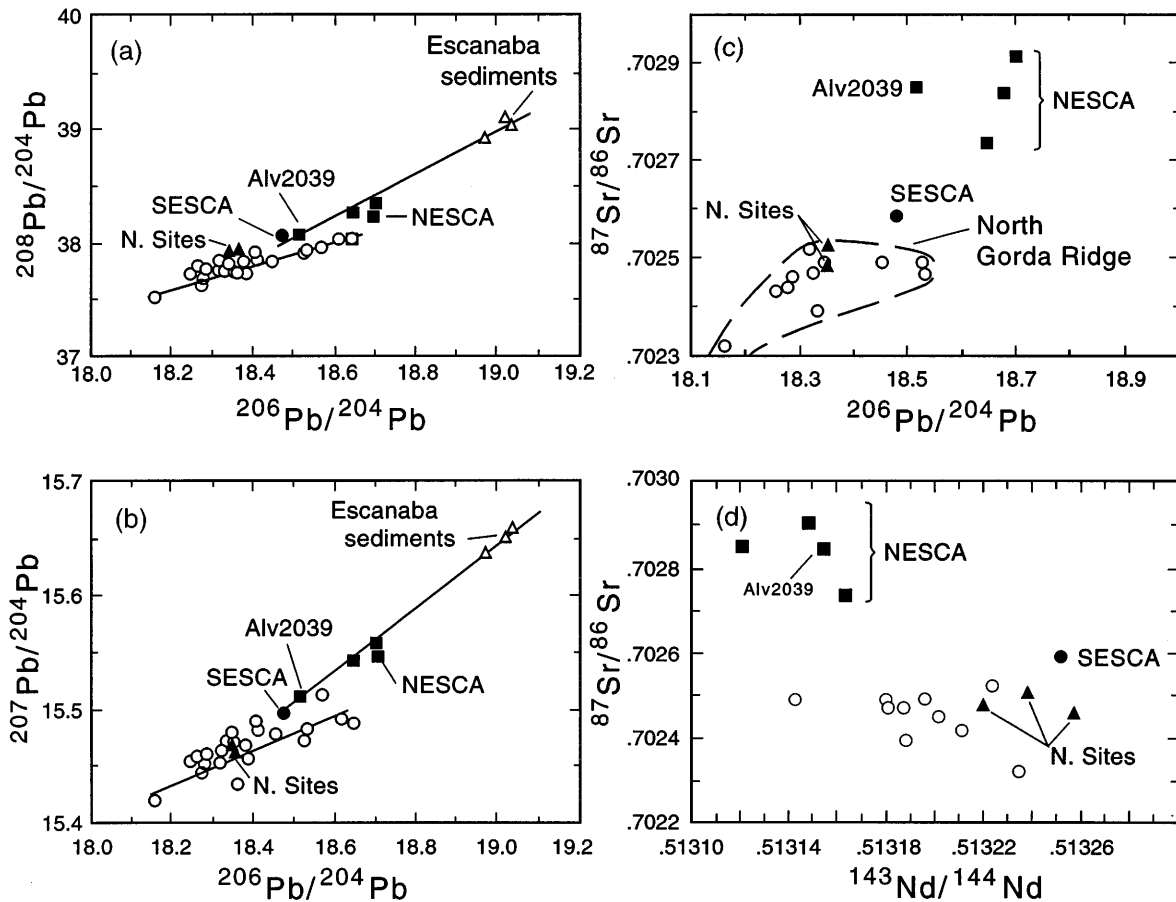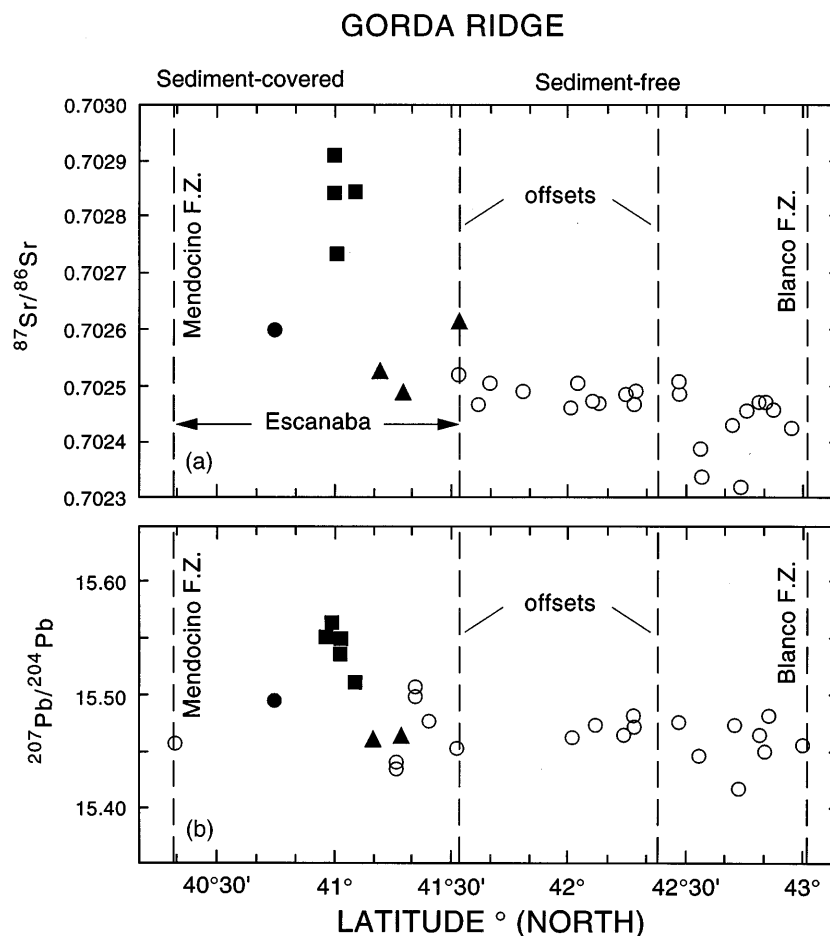
Fig. 6. Isotopic compositions of Escanaba basalts in comparison with basalts from the northern Gorda Ridge. (a) $^{208}Pb/^{204}Pb$ vs $^{206}Pb/^{204}Pb$ and (b) $^{207}Pb/^{204}Pb$ vs $^{206}Pb/^{204}Pb$ show samples from the NESCA site (■) displaced toward the composition of local sediments (△). (c) $^{87}Sr/^{86}Sr$ vs $^{206}Pb/^{204}Pb$ shows higher Sr isotopic ratios that are not well correlated with Pb for NESCA samples. The SESCA sample (●) has slightly higher $^{87}Sr/^{86}Sr$ than basalts from the northern Gorda Ridge (○). (d) $^{87}Sr/^{86}Sr$ vs $^{143}Nd/^{144}Nd$ shows NESCA basalts with higher Sr and lower Nd isotopic ratios than other Gorda Ridge basalts. Data for northern Gorda Ridge from Church & Tatsumoto (1975), White *et al.* (1987), and W. M. White (unpublished data, 1990). Data for sediment from LeHuray *et al.* (1987) and R. Bouse (unpublished data, 1990). North Pacific sediments are not shown in (c) and (d) because their $^{87}Sr/^{86}Sr$ (>0·71) values plot so far off field.

complex petrogenetic processes. Only the unfractionated basalt (*mg*-number 66·7) from the northern Escanaba site has a LREE concave-downward N-MORB profile that is typical for northern Gorda Ridge basalt. The SESCA sample, although it is comparably unfractionated (*mg*-number 66·2), has a flatter, less depleted LREE profile and a significant negative Eu anomaly. The NESCA samples have highly variable crossing REE patterns although they are within a narrow fractionation range (*mg*-number 60–57). Complex crossing REE pattern can be produced by complex melting processes, which, however, would not change isotopic ratios.

Isotopic ratios mirror the REE patterns showing highly variable, radiogenically enriched compositions for the NESCA site. The isotopic compositions of the samples from the northern sites indicate a highly depleted source similar to that of northern Gorda Ridge basalts. The unfractionated SESCA sample is isotopically slightly more enriched than northern Gorda Ridge basalt but the NESCA samples have the highest Sr and Pb and the lowest Nd isotopic ratios observed for any samples from the Gorda Ridge (Fig. 6). Although there are minor variations in isotopic compositions for northern Gorda Ridge basalts, all indicate a slightly heterogeneous but highly depleted N-MORB source (Fig. 7). Even the most fractionated composition (83-16a) from the most northerly site in Escanaba Trough, which has a K₂O comparable with most of the NESCA samples, has a low $^{87}Sr/^{876}Sr$ of 0·70261 (Table 2). It is possible that the NESCA basalts have a more enriched source that is highly heterogeneous on a very small scale; alternatively, the observed variations may be due to shallow processes.

Chlorine studies of MORB magmas (Michael & Schilling, 1988; Michael & Cornell, 1996) have shown

GORDA RIDGE

Fig. 7. Variation in (a) $^{87}Sr/^{86}Sr$ and (b) $^{207}Pb/^{204}Pb$ with latitude for the entire Gorda Ridge shows distinct isotopic enrichment for the NESCA site. The isotopic composition of the SESCA basalt falls within the range of compositions of other Gorda Ridge basalt, although it is on the high end of the spectrum. Symbols and data sources as in Fig. 6; additional Sr isotopic data from Davis & Clague (1987).

convincingly that MORB magmas may be affected by crustal processes and assimilate small amounts of hydrothermally altered oceanic crust. As the compositional contrast between magma and wall rocks composed of the oceanic crust is small, contamination effects are very subtle. At Escanaba Trough, magma intrudes, and apparently ponds, beneath a thick sediment cover with distinctively different compositions. As a result of the difference in density, basaltic magma may form pods and sills at the base of the sediment sequence, as inferred from seismic reflectors (Zierenberg *et al.*, 1994). Abundance of faults and fissures of the extensional environment may allow eruption through the sediment cover.

The sediments have a lower melting point than the oceanic crust and much higher Sr and Pb isotopic ratios. Pb isotopic ratios are most sensitive to sediment contamination and the Escanaba Pb isotopic compositions are displaced toward that of sediment (Fig. 6). Sr isotopic

compositions of NESCA samples are also significantly enriched over northern Gorda Ridge basalts. However, small amounts of seawater alteration can significantly alter Sr isotopic ratios. The $^{87}Sr/^{86}Sr$ ratio of the glass from Alv2039-2 may have been affected by seawater alteration as the lava interacted with wet sediment. The elevated $\delta^{18}O$ of the glass compared with the interior of the rock suggests some low-temperature surface alteration, as does the inhomogeneous Cl of the glass rind. The Pb isotopic composition of this sample, which is poorly correlated with the Sr isotopic ratio, was probably not affected by surface alteration because Pb concentration in seawater is very low. The oxygen isotopic ratios of the other glasses are typical for MORB, although an unreasonable amount of assimilation would be required to significantly alter the $\delta^{18}O$.

The small trace element and isotopic enrichment shown by the SESCA sample may also have resulted from

Table 3: Analyses of sediment from Escanaba Trough

Sample:	L2-86-14-7	L2-86-9G-105	L1-86-211-212	DSDP35-14-1
	Silty clay	Silty clay	Silty clay	Siltstone
(wt %)				
SiO_2	53·0	30·3	58·5	73·7
Al_2O_3	16·5	20·7	15·5	12·1
FeO^T	12·4	10·1	7·04	2·64
MnO	0·10	0·04	0·20	1·06
MgO	3·75	25·5	3·74	2·85
CaO	0·76	0·10	2·84	2·92
Na_2O	1·75	0·30	2·28	2·17
K_2O	2·17	0·03	2·56	0·34
P_2O_5	0·20	0·06	0·22	0·18
TiO_2	0·80	1·12	0·78	0·03
LOI	7·61	11·7	6·01	1·58
Total	99·0	100·0	99·7	99·6
(ppm)				
La	33	44	29	25
Ce	65	83	58	49
Nd	29	38	27	21
Sm	5·1	7·1	4·8	3·4
Eu	1·9	1·8	1·2	0·95
Tb	0·76	0·99	0·69	0·47
Yb	2·3	3·3	2·3	1·6

FeO^T is total Fe calculated as FeO. Major elements by XRF, REE by ICP-MS analysis. LOI, loss on ignition at 950°C.

sediment contamination, as this sample also erupted through a thick sediment cover. However, because of the unfractionated nature of the sample, the effects are very subtle. Assimilation would be minimal if magma ascended rapidly and spent little time fractionating in the crust.

ASSIMILATION–FRACTIONATION MODELS

Taylor (1980) and DePaolo (1981) first showed that assimilation and fractional crystallization should be viewed as a coupled process, with the heat required for assimilation provided by the latent heat of crystallization of the magma. The amount of assimilation will depend on physical parameters such as temperature contrast between magma and wall rock, rate of magma ascent, amount of fractional crystallization, and fusion temperature of the wall rock. One effect of assimilation is to speed up formation of cumulus mineral phases, driving the process in the same direction as it would have gone anyway. However, AFC processes may deviate

significantly from simple binary mixing depending on the bulk–liquid distribution coefficients.

We have constructed AFC models for Escanaba Trough lavas using the equation of DePaolo (1981):

$$Cm = C^o\{F - z + [(r/r - 1)(Ca/zC^o)(1 - F - z)]\}$$

where Cm is the concentration of the element in the contaminated magma, C^o is the concentration in the original magma, Ca is the concentration in the assimilant, F is the fraction of liquid remaining after crystallization, r is Ma/Mc, the ratio of mass assimilated to the mass crystallized, and $z = (r + D - 1)/(r - 1)$, where D is the bulk liquid distribution coefficient.

For the AFC calculations for Pb, we used a parental magma Pb concentration of 0·5 ppm, based on the analyses of Church & Tastumoto (1975) and White (1993), and the depleted isotopic ratios of the sample (3-86-2) from the northern site. For the assimilant, we used the isotopic composition of NESCA sediment (Alv2039-1A) of LeHuray *et al.* (1987), and a Pb concentration of 42 ppm, which is the average of >100 sediment analyses of Karlin & Lyle (1986), omitting near-surface samples

which have >100 ppm Pb. A bulk distribution coefficient (*D*) for Pb of 0·6 was used based on an average *D* for plagioclase–liquid (0·18–1·07; Dunn & Sen, 1994). Plagioclase is the only phase crystallizing in the observed fractionation range that would exert strong control on the bulk liquid distribution coefficient, as *D* values for clinopyroxene and olivine are extremely low. The steep asymptotic curves generated (Fig. 8a) show that isotopic ratios increase rapidly over the applicable fractionation range (25–40%) without significantly changing the Pb concentrations in the magma (<2 ppm). A ratio (*r*) of assimilant to fractionating crystals of 0·03 gives the best fit, suggesting assimilation of ~1·2% sediment. Using an assimilant with only 17 ppm Pb, the lowest concentration observed in NESCA sediment (Karlin & Lyle, 1986) would require a little over 2% of sediment. This is in close agreement with simple binary mixing which indicates ~2·5% sediment.

AFC calculation for Nd (Fig. 8b) shows that Nd isotopic ratios are much less sensitive to sediment assimilation and generate flatter curves with Nd concentrations in the magma increasing more rapidly for smaller changes in the isotopic ratio. Again, for the initial magma the Nd concentration and isotopic ratio of the unfractionated sample from the northern Escanaba site was used. As Sr and Nd isotopic compositions were not determined for the Escanaba sediment, we used a North Pacific sediment composition of Cousens *et al.* (1994) with 60 ppm Nd abundance and an isotopic ratio of 0·51249 for the sediment assimilant. A *D* of 0·06 was used based on calculated bulk liquid distribution coefficient of Perfit *et al.* (1983) for Galapagos basalt. Using a smaller *D* tends to further flatten the curve, increasing the concentrations of Nd in the magma more rapidly for small changes in isotopic ratios. Using a smaller *r* value has the same effect as decreasing *D*. Although there is no single curve that matches all of the Escanaba compositions, assimilation of ~1·5% sediment is in general agreement with the Pb data.

AFC processes involving Sr are even more complicated because the distribution coefficient of Sr can change more significantly in a fractionating magma than the *D* values for Nd and Pb in the compositional range observed at Escanaba Trough. For *D* <1, a similar pattern to Nd is observed with Sr concentrations increasing concurrently with the isotopic ratio. However, with *D* >1 the Sr isotopic ratio can change dramatically and the concentration of Sr in the magma can actually decrease below that of the assimilant (Fig. 8c). For the fractionation range observed in the Escanaba basalt, Sr undoubtedly behaved as an incompatible element. Most of these samples were not analyzed for Sr, but the basalts from the northern Gorda Ridge show an increase in Sr over a comparable fractionation range (fig. 5c of Davis & Clague, 1987) indicating that Sr behaved incompatibly for the observed

fractionation range. Using *D* = 0·4 and *r* = 0·03, NESCA basalt (6-85-36) composition suggests assimilation of ~1·2% sediment, in reasonable agreement with the Pb and Nd data. However, the Sr concentration of Alv2039-2, with a comparable *mg*-number and identical Sr isotopic ratio, does not fit using the same parameters, suggesting different assimilant composition and/or different *D* and *r* values.

The parameters can be varied to give slightly different results; however, the modeling shows that with a range of reasonable parameters the NESCA basalt compositions can be generated from a depleted N-MORB magma like that at the northern site by assimilating 1–2% of sediment. With a slightly more enriched source or a more enriched assimilant even smaller amounts of sediment can produce the same effects. Although AFC processes can significantly alter some trace element and isotopic ratios for such small amounts of assimilation, major element concentration would not be notably altered. All of the glasses from NESCA have slightly higher SiO_2 than other Gorda glasses but values are still well within analytical precision. As assimilation and fractionation are coupled processes, the mineral composition may also show subtle changes. The higher K_2O in plagioclase of Alv2039-2 and the higher ferric iron content of the abundant spinel in NESCA lavas, indicating higher oxygen fugacity (Fig. 3), are probably such subtle signals that they would normally be dismissed as analytical noise. Overenrichment in elements such as Cl, Th, and LREE, which are present in very low concentrations in MORB, and shifts in isotopic compositions toward sediment may simulate enriched source characteristics. Small-scale heterogeneities observed in some other MORB suites may also have resulted from reaction with and assimilation of wall rock, but because of greater compositional similarity between magma and wall rock, composed of hydrothermally altered oceanic crust, the effects may be very subtle. The effects of crustal contamination should be carefully evaluated when attributing small-scale heterogeneities in MORB to differences in mantle sources, especially at sediment-covered ridges.

Fig. 8. AFC models for Escanaba basalt showing changes in composition of a depleted N-MORB parental magma (3-86-2) as a result of concurrent fractional crystallization and assimilation of sediment. (a) $^{206}Pb/^{204}Pb$ ratios increase rapidly for only small shifts in Pb concentration in the contaminated magma. (b) $^{143}Nd/^{144}Nd$ ratios show much smaller changes for larger shifts in Nd concentrations. (c) $^{87}Sr/^{86}Sr$ and Sr concentration changes at variable *D* values of 0·4, 1·0, and 2·0. For *D* <1, isotopic ratios and Sr concentrations increase but for *D* >1 the isotopic ratio increases rapidly with only a small increase or even a decrease in the Sr concentration in the contaminated magma. Path for simple crystal fractionation is indicated (SFC). Symbols as in Fig. 6.
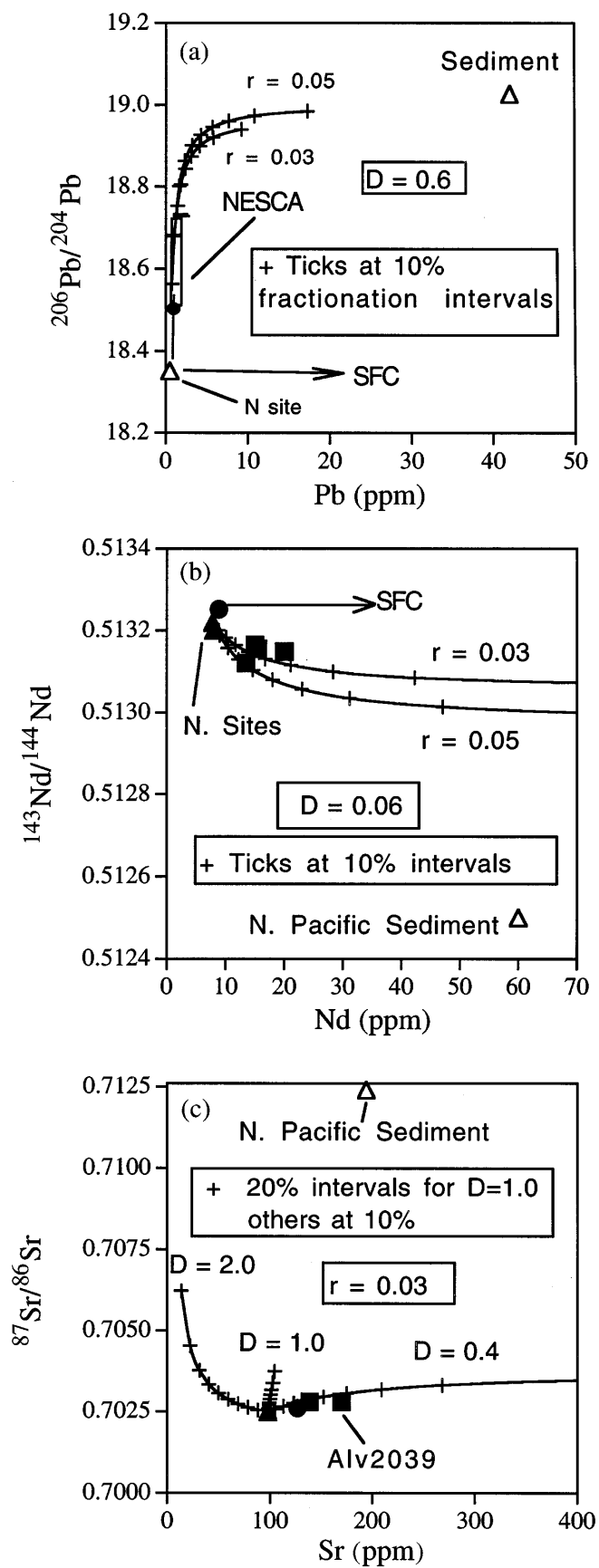
Fig. 8.

DISCUSSION

Ocean island basalt magmas have less depleted incompatible element and isotopic compositions and hence the contrast between magma and wall rock is smaller than in the case presented here, making it more difficult to detect small amounts of assimilation in the basalt compositional range. Elevated Cl contents (Clague *et al.*, 1995) and low oxygen isotope ratios (Kyser *et al.*, 1982; Eiler *et al.*, 1996) in ocean island basalts have been interpreted as resulting from assimilation of hydrothermally altered wall rock from the oceanic crust or from the volcanic edifice. With more extensive fractionation in the mugearite to trachyte compositional range, assimilation of crustal material becomes more pronounced. Distinctive negative Ce anomalies and changes in incompatible element ratios such as Ba/Nb, Ce/Pb in evolved ocean island basalt have been attributed to crustal contamination (Bohrson & Reid, 1995; Thirlwall *et al.*, 1997). These observations demonstrate that extensive crystal fractionation is accompanied by more extensive assimilation, which amplifies the geochemical signature of assimilation. Hence, studies that seek to identify heterogeneities in mantle source rocks for MORB and ocean island basalts should rely most strongly on the chemical compositions of the least fractionated samples. High *mg*-numbers of whole-rocks do not invariably identify such unfractionated lavas, as many MORB and ocean island basalts contain abundant accumulated crystals (xenocrysts). High *mg*-number of the glass, which represents the quenched melt, is the defining characteristic of unfractionated lava.

In oceanic island lavas, the assimilant is more likely to be altered oceanic crust or altered volcanic rocks that make up the volcanic edifice, rather than sediment because these lavas are not erupted in an extensional setting with thick sediment cover. However, given the tectonic setting in which Escanaba basalt erupted, stoping and assimilation of small amounts of sediment by the denser magma ponding beneath the sediment cover is to be expected, if not inevitable. Given the density differences between magma and sediment, without extension along faults and deep fissures eruption through thick sediment may not be possible. Considering the diversity of the sediment compositions observed in Escanaba Trough, assimilation of even very small amounts of sediment can generate the chemical variations observed from a common N-MORB parental magma. However, further complexity may be introduced if assimilation of partially melted sediments or fluids that have equilibrated with sediment were involved, instead of, or in addition to, assimilation of bulk sediment. Chemical changes that may be caused by shallow processes, particularly assimilation, need to be considered when evaluating petrogenesis of even MORB magmas.

CONCLUSIONS

MORBs from Escanaba Trough show small but significant enrichment in incompatible elements and Sr and Pb isotopic ratios for samples from the sediment-covered, southern segment of the trough. Basalt from the sediment-free northern sites in Escanaba Trough have depleted N-MORB compositions similar to those typical on the northern Gorda Ridge. Although major element chemistry of basalt from the sediment-covered ridge segment is similar, LREE abundances and Sr and Pb isotopic ratios are higher and Nd significantly lower than for other samples recovered from the Gorda Ridge. Sr and Pb isotopic ratios are shifted toward the composition of sediments; Pb isotopic ratios, in particular, fall on a mixing trend with local sediments. AFC mixing calculations suggest that 1–2% assimilation of local sediments could produce the enrichment trend observed for some NESCA basalts, if depleted N-MORB parental magmas similar to those from the sediment-free, northern sites are assumed. Compositional variability in the sediments present in the trough might account for the observed variability and poor correlations for some elements and isotopic ratios in the lavas, although we suspect that selectively melted small percentages of sediment and/or a fluid phase, equilibrated with sediments, may have been involved.

Small-scale variations in MORB chemistry, especially on a local scale, can be caused by assimilation of sediment, and perhaps of altered, volcanic wall rock and may not invariably indicate heterogeneous mantle sources. The strong compositional contrast between depleted N-MORB magma and sediment makes it possible to detect crustal contamination. These observations suggest that crustal processes may produce subtle chemical changes in oceanic basalt magmas that need to be considered when evaluating petrogenesis of oceanic volcanic rocks.

REFERENCES

Atwater, T. & Mudie, J. D. (1973). Detailed near-bottom geophysical study of the Gorda Rise. *Journal of Geophysical Research* **78,** 8665–8686.

Bohrson, W. A. & Reid, M. R. (1995). Petrogenesis of alkaline basalts from Socorro Island, Mexico: trace element evidence for contamination of ocean island basalt in the shallow ocean crust. *Journal of Geophysical Research* **100,** 24555–24576.

Bohrson, W. A., Davidson, J. & Wolff, J. A. (eds) (1996). *Shallow Level Processes in Ocean Island Magmatism.* Chapman Conference, Tenerife, Canary Islands. Washington, DC: American Geophysical Union, p. 25.

Church, S. E. & Tatsumoto, M. (1975). Lead isotope relations in oceanic ridge basalts from the Juan de Fuca–Gorda Ridge area, N.E. Pacific Ocean. *Contributions to Mineralogy and Petrology* **53,** 253–279.

Clague, D. A., Moore, J. G., Dixon, J. E. & Friesen, W. B. (1995). Petrology of submarine lavas from Kilauea's Puna Ridge, Hawaii. *Journal of Petrology* **36,** 299–349.

Clayton, R. N. & Mayeda, T. K. (1963). The use of bromine pentafluoride in the extraction of oxygen from oxides and silicates for isotopic analyses. *Geochimica et Cosmochimica Acta* **27,** 43–52.

Cousens, B. L., Allan, J. F. & Gorton, M. P. (1994). Subduction-modified pelagic sediments as the enriched component in back-arc basalts from the Japan Sea: Ocean Drilling Program Sites 797 and 794. *Contributions to Mineralogy and Petrology* **117,** 421–434.

Davis, A. S. & Clague, D. A. (1987). Geochemistry, mineralogy, and petrogenesis of basalt from the Gorda Ridge. *Journal of Geophysical Research* **92,** 10467–10483.

Davis, A. S. & Clague, D. A. (1990). Gabbroic xenoliths from the northern Gorda Ridge: implications for magma chamber processes under slow-spreading centers. *Journal of Geophysical Research* **95,** 10885–10990.

Davis, A. S., Clague, D. A. & Friesen, W. B. (1994). Petrology and mineral chemistry of basalt from Escanaba Trough, southern Gorda Ridge. *US Geological Survey Bulletin* **2022,** 153–170.

Denlinger, R. P. & Holmes, M. L. (1994). A thermal and mechanical model for sediment hills and associated sulfide deposits along Escanaba Trough. *US Geological Survey Bulletin* **2022,** 65–75.

DePaolo, D. J. (1981). Trace element and isotopic effects of combined wallrock assimilation and fractional crystallization. *Earth and Planetary Science Letters* **53,** 189–202.

Dunn, T. & Sen, C. (1994). Mineral/matrix partition coefficients for orthopyroxene, plagioclase, and olivine in basaltic to andesitic systems: a combined analytical and experimental study. *Geochimica et Cosmochimica Acta* **58,** 717–733.

Eiler, J. M., Farley, K. A., Valley, J. W., Hofmannn, A. W. & Stolper, E. M. (1996). Oxygen isotope constraints on the sources of Hawaiian volcanism. *Earth and Planetary Science Letters* **53,** 453–468.

Glazner, A. F., Farmer, G. L., Hughes, W. T., Wooden, J. L. & Pickthorn, W. (1991). Contamination of basaltic magma by mafic crust at Amboy and Pisgah Craters, Mojave Desert, California. *Journal of Geophysical Research* **96,** 13673–13691.

Goldstein, S. J., Murrell, M. T., Janecky, D. R., Delaney, J. R. & Clague, D. A. (1992). Geochronology and petrogenesis of young MORB from the Juan de Fuca and Gorda Ridges by ^{238}U–^{230}Th disequilibrium. *Earth and Planetary Science Letters* **109,** 255–272.

Haskin, L. A., Frey, F. A., Schmitt, R. A. & Smith, R. H. (1968). Meteoric, solar, and terrestrial rare-earth distributions. *Physics and Chemistry of the Earth* **7,** 167–321.

Karlin, R. & Lyle, M. (1986). Sediment studies on the Gorda Ridge. Open-File Report 0-86-19. Portland, OR: State of Oregon Department of Geology and Mineral Industries, 76 pp.

Kyser, T. K., O'Neil, J. R. & Carmichael, I. S. E. (1982). Genetic relations among basic lavas and ultramafic nodules: evidence from oxygen isotope compositions. *Contributions to Mineralogy and Petrology* **81,** 88–102.

Leeman, W. P. & Hawkesworth, C. J. (1986). Open magma systems: trace element and isotopic constraints. *Journal of Geophysical Research* **91,** 5901–5912.

LeHuray, A. P., Church, S. E., Koski, R. A. & Bouse, R. M. (1987). Pb isotopes in sulfides from mid-ocean ridge hydrothermal sites. *Geology* **16,** 362–365.

Lichte, F. E., Meier, A. L. & Crock, J. G. (1987). Determination of the rare-earth elements in geological material by inductively coupled plasma mass spectrometry. *Analytical Chemistry* **59,** 1150–1157.

McManus, D. A. (1970). Site 35. In: McManus, D. A. *et al.* (eds) *Initial Reports of the Deep Sea Drilling Project, 5.* Washington, DC: US Government Printing Office, pp. 165–172.

Michael, P. J. & Cornell, W. C. (1996). Assimilation beneath ocean islands: inferences from mid-ocean ridge basalts. In: Bohrson, W. A., Davidson, J. & Wolff, J. A. (eds) *Shallow Level Processes in Ocean Island Magmatism.* Chapman Conference, Tenerife, Canary Islands. Washington, DC: American Geophysical Union, p. 25.

Michael, P. J. & Schilling, J. G. (1988). Chlorine in mid-ocean ridge magmas: evidence for assimilation of seawater-influenced components. *Geochimica et Cosmochimica Acta* **53,** 3131–3143.

Moore, G. W. & Sharman, G. F. (1970). Summary of scan Site 4. In: McManus, D. A. *et al.* (eds) *Initial Reports of the Deep Sea Drilling Project, 5.* Washington, DC: US Government Printing Office, pp. 761–773.

Morton, J. L. & Fox, C. G. (1994). Structural setting and interaction of volcanism and sedimentation at Escanaba Trough: geophysical results. *US Geological Survey Bulletin* **2022,** 21–43.

Perfit, M. R., Fornari, D. J., Malahoff, A. & Embley, R. W. (1983). Geochemical studies of abyssal lavas recovered by DSRV *Alvin* from eastern Galapagos Rift, Inca Transform, and Ecuador Rift. 3. Trace element abundances and petrogenesis. *Journal of Geophysical Research* **88,** 10551–10572.

Riddihough, R. P. (1980). Gorda plate motions from magnetic anomaly analysis. *Earth and Planetary Science Letters* **51,** 163–170.

Ross, S. L. & Zierenberg, R. A. (1994). Volcanic geomorphology of the SESCA and NESCA sites, Escanaba Trough. *US Geological Survey Bulletin* **2022,** 143–152.

Sigurdsson, H. & Schilling, J. G. (1976). Spinels in Mid-Atlantic Ridge basalts: chemistry and occurrence. *Earth and Planetary Science Letters* **29,** 7–20.

Taylor, H. P. (1980). The effects of assimilation of country rocks by magmas on ^{18}O/^{16}O and ^{87}Sr/^{86}Sr systematics in igneous rocks. *Earth and Planetary Science Letters* **47,** 243–254.

Thirlwall, M. F., Jenkins, C., Vroon, P. Z. & Mattey, D. P. (1997). Crustal interaction during construction of ocean islands: Pb–Sr–Nd–O isotope geochemistry of the shield basalts of Gran Canaria, Canary Islands. *Chemical Geology* **135,** 233–262.

Vallier, T. L., Harold, P. J. & Girdley, W. A. (1973). Provenances and dispersal patterns of turbidite sand in Escanaba Trough, northeastern Pacific Ocean. *Marine Geology* **15,** 67–87.

White, M. W., Hofman, A. W. & Puchelt, H. (1987). Isotope geochemistry of Pacific mid-ocean ridge basalt. *Journal of Geophysical Research* **92,** 4881–4893.

White, W. M. (1993). ^{238}U/^{204}Pb in MORB and open system evolution of the depleted mantle. *Earth and Planetary Science Letters* **115,** 211–226.

White, W. M., Cheatham, M. M. & Duncan, R. A. (1990). Isotope geochemistry of Leg 115 basalts and inferences on the history of the Reunion mantle plume. In: Duncan, R. A. *et al.* (eds) *Proceedings of the Ocean Drilling Program, Scientific Results, 115B.* College Station, TX: Ocean Drilling Program, pp. 53–61.

Zierenberg, R. A. & Shanks, W. C. III (1994). Sediment alteration associated with massive sulfide formation in Escanaba Trough, Gorda Ridge: the importance of seawater mixing and magnesium metasomatism. *US Geological Survey Bulletin* **2022,** 257–278.

Zierenberg, R. A., Morton, J. L., Koski, R. A. & Ross, S. L. (1994). Geologic setting of massive sulfide mineralization in Escanaba Trough. *US Geological Survey Bulletin* **2022,** 171–197.